Establishment of a mouse model for bile duct repair and tissue engineering

XINLAN GE[1*], DABIN XU[2*], KE PAN[1], GUANKUN MAO[1], SHICHUN LU[2] and CHONGHUI LI[1]

[1]Institute of Hepatobiliary Surgery and [2]Faculty of Hepato-Pancreato-Biliary Surgery, Chinese PLA General Hospital, Beijing 100853, P.R. China

Received July 21, 2022; Accepted October 13, 2022

DOI: 10.3892/etm.2022.11675

Abstract. Due to the lack of a suitable model, research on biliary biology is far behind that on other organs. A mouse model of common bile duct (CBD) dilation (BDD) was first established and compared with CBD ligation mice (BDL). Then, in a transplantation experiment, the dilated CBD of recipient BDD mice was injured by making an elliptical incision and repaired by transplanting a bile duct patch from donor BDD mice. Biochemical and histological changes were analyzed and cell proliferation of the bile duct grafts was determined. Slightly dilated and unblocked CBD with a diameter of 2.89±0.76 mm was obtained in BDD mice, while the CBD diameter was 0.51±0.08 mm in the Sham group and 4.71±0.64 mm in the BDL group on day 14 after surgery. The liver damage was very mild in BDD mice compared with BDL mice, proving that the BDD model could be further used for bile duct transplantation. By cross transplanting the bile duct patch from enhanced green fluorescence protein and wild-type BDD mice, it was found that the CBD injury was well repaired and the cells of the bile duct patch were completely replaced by recipient-derived cells at 12 week after the repair operation. α Smooth muscle actin, Ki67 and cytokeratin 19 immunofluorescence staining showed that the proliferation of bile duct epithelial cells and abundant active fibroblasts were found within the bile duct patch during the regeneration process. Therefore, a reliable new mouse model of bile duct injury and repair was successfully established and can be used in the study of biliary repair mechanisms and tissue engineering of biliary ducts.

Correspondence to: Professor Shichun Lu, Faculty of Hepato-Pancreato-Biliary Surgery, Chinese PLA General Hospital, 28 Fuxing Road, Beijing 100853, P.R. China
E-mail: lsc620213@aliyun.com

Dr Chonghui Li, Institute of Hepatobiliary Surgery, Chinese PLA General Hospital, 28 Fuxing Road, Beijing 100853, P.R. China
E-mail: Lich_plagh@163.com

*Contributed equally

Key words: bile duct injury, bile duct repair, regeneration, mouse model, tissue engineering

Introduction

Iatrogenic bile duct injury is a serious and potentially life-threatening complication of cholecystectomy (1). Improper management of bile duct injury and traumatic bile duct stricture leads to severe consequences, such as repeated cholangitis, formation of hepatolithiasis and biliary cirrhosis (2). Bile duct injury seriously affects the quality of life of patients (3). At present, surgery is the main treatment for the injured bile duct. Roux-en-Y hepaticojejunostomy has been the most commonly used approach for biliary reconstruction. However, because this operation changes the physiological structure of the biliary tract, its long-term outcome is still far from satisfactory due to the high incidence of reflux cholangitis, choledocholithiasis, biliary cirrhosis, anastomotic stenosis and even oncogenesis (4,5).

Tissue-engineered bile ducts can potentially be used for repairing bile duct injury while preserving the function of the Oddi sphincter. New techniques in bile duct epithelial organoids culture and cell reprogramming provide a new opportunity in the regenerative medicine of bile duct (6). Sampaziotis *et al* (7) seeded human cholangiocyte organoids (ECOs) on a biodegradable scaffold to form artificial structure and to repair the gallbladder wall or bile duct in immunodeficiency mice. They proved the potential of ECOs in bile duct repair. However, if the exogenous cells seeded in the tissue-engineered bile ducts could survive in healthy animals but not immunodeficiency animals still needs evidence. Several studies in pigs or dogs have shown that transplanted acellular artificial bile duct scaffolds could be re-epithelialized but lack experimental details (8,9). In clinical studies, the application of autologous graft to repair bile duct defects also failed to demonstrate whether biliary re-epithelialization occurred due to ethical issues (10). However, preliminary evidence demonstrates that recipient-derived cells are observed in the peribiliary glands and biliary epithelium of the large donor bile ducts after liver transplantation (11). Notably, it is worth investigating whether it is possible to perform bile duct allografts, as in vascular surgery (12,13).

Mice are the most commonly used laboratory animals and various transgenic and gene knockout mice can provide

beneficial technical means for in-depth research on the repair mechanism of biliary tract injury. To establish a reproducible mouse model that can be used for bile duct repair research, the present study used the partial bile duct ligation technique (14) to cause common bile duct (CBD) distal stenosis and proximal dilation (i.e., bile duct dilation, BDD). Then, it developed a microsurgical operation for bile duct injury and repair of the dilated bile duct. The present study proved the feasibility and safety of this novel model for bile duct injury and repair research in mice.

Materials and methods

Animals. Adult male C57BL/6 mice (n=85; age, 8 to 10 weeks; weight, 20-24 g) were purchased from Beijing Vital River Laboratory Animal Technology Co., Ltd. Twenty adult male C57BL/6-Tg [CAG-enhanced green fluorescence protein (EGFP)]/Nju mice (age, 8 to 10 weeks; weight, 20-24 g) were purchased from Nanjing University Model Animal Center. Animals were fed standard chow with water *ad libitum* and kept at 24˚C and 40% humidity with a 12 h light/dark cycle. Experiments were approved by the Committee on Ethics of Animal Experiments of the Chinese PLA General Hospital (approval no. 2017-X13-65) and in compliance with the recommendations of the Guide for the Care and Use of Laboratory Animals of the National Research Council (US) Committee, 8th edition, 2011 (https://nap.nationalacademies.org/read/12910).

Experimental design. In the BDD model experiment (Fig. 1), C57BL/6 mice were randomly divided into three groups: A control group with a sham operation (Sham group; n=6), a bile duct dilation group with a CBD partial ligation to cause CBD distal stenosis and proximal dilation (BDD group; n=24) and a bile duct ligation group with CBD ligated (BDL group; n=24). The BDD and BDL groups were set to three time points: 7, 14 and 21 days after the operation (n=8 for each time point in each group). Each mouse was weighed preoperatively (day 0) and on days 7, 14 and 21 after the operation. The mouse with body weight loss >20% was sacrificed by exsanguination under 3% isoflurane anesthesia before the planned time point (15). All mice were monitored every day for their health and behavior in our Experimental Animal Centre.

In the bile duct injury and repair experiment (Fig. 1), an elliptical incision was made in the anterior wall of the dilated CBD of recipient BDD mice and then repaired by transplanting a bile duct patch from donor BDD mice. The patches from EGFP mice were transplanted into wild-type mice (EGFP donors: n=14; C57BL/6 recipients: n=28) and the patches from wild-type mice were transplanted into EGFP mice (C57BL/6 donors: n=3; EGFP recipients: n=6). One donor could provide bile duct patches for two recipients. Four time points (1, 2, 4 and 12 weeks after transplantation) were set to observe the outcomes of recipient mice.

Surgery for the BDD mouse model. All mice were fasted overnight with free access to water before surgery. Anesthesia was performed under isoflurane/oxygen inhalation (3% isoflurane for induction, 1.5% for maintenance of anesthesia). Following a midline incision, the CBD was exposed and separated

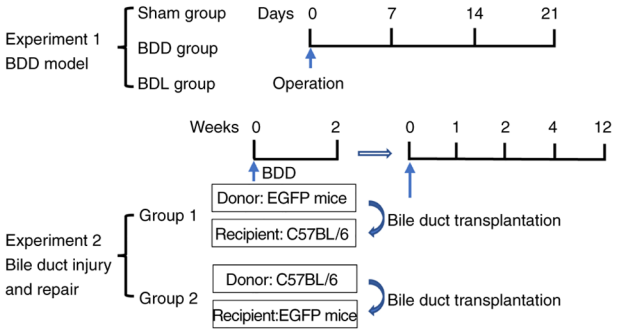

Figure 1. A schematic graph of the experimental design and groups. BDD, bile duct dilation; BDL, bile duct ligation; EGFP, enhanced green fluorescence protein.

carefully by a microtweezer under a surgical microscope. In the Sham group, the abdomen was closed after the CBD was separated (Fig. 2A). In the BDD group, an 8-0 nylon suture was placed around the CBD at the upper edge of the pancreas and tied with one lax surgical knot. An 8-0 surgical needle (Φ=0.15 mm, Nylon suture; Lingqiao) was placed into the lax surgical knot (Fig. 2B) and then the knot was tied tightly (Fig. 2C). The needle was removed, leaving a defined lumen between the bile duct and the ligation suture (Fig. 2D). The superfluous sutures were removed with a microscissor and the abdomen was closed by a 4-0 surgical suture. In the BDL group, the CBD was ligated tightly with two surgical knots using 8-0 nylon suture and then the CBD was transected between the two knots (Fig. 2E).

Surgery for bile duct injury and repair. At 14 days after the modelling operation, BDD mice were used as donors and recipients. First, the dilated CBD of donor mice was excised, divided into two patches and stored in a histidine-tryptophan-ketoglutarate solution (Custodiol, Koehler Chemi) at 4˚C for transplantation. Second, the dilated CBD of recipient mice was exposed (Fig. 2F). An elliptical incision of ~2x3 mm was made with a microscissor on the ventral side of the CBD (Fig. 2G). The bile was absorbed with a cotton swab. A donor patch was taken and trimmed to be slightly larger than the incision. The patch was first fixed to the CBD at the upper and lower ends with two sutures using two 8-0 nylon threads with needles and then continuous suture was performed from the top to the bottom at one side and from the bottom to the top at the other side of the patch (Fig. 2H). After ensuring no bile leakage, the abdominal cavity was rinsed with normal saline and the abdomen was closed with a 4-0 suture. Antibiotics (cefoperazone sulbactam sodium; Pfizer, Inc.; 60 mg/kg, once per day) were given for 3 days postoperatively and 20% glucose in their drinking water was given for 24 h except for the standard laboratory chow *ad libitum* (16).

Sample collection and CBD diameter measurement. The mice were anaesthetized with isoflurane (3% isoflurane for induction, 1.5% for maintenance of anesthesia) and the abdomen was opened by a midline incision. The diameter of the CBD was measured *in situ* with a Vernier caliper. Blood was collected via the vena cava with a 1 ml syringe. The CBD was perfused with 4% paraformaldehyde via the gallbladder.

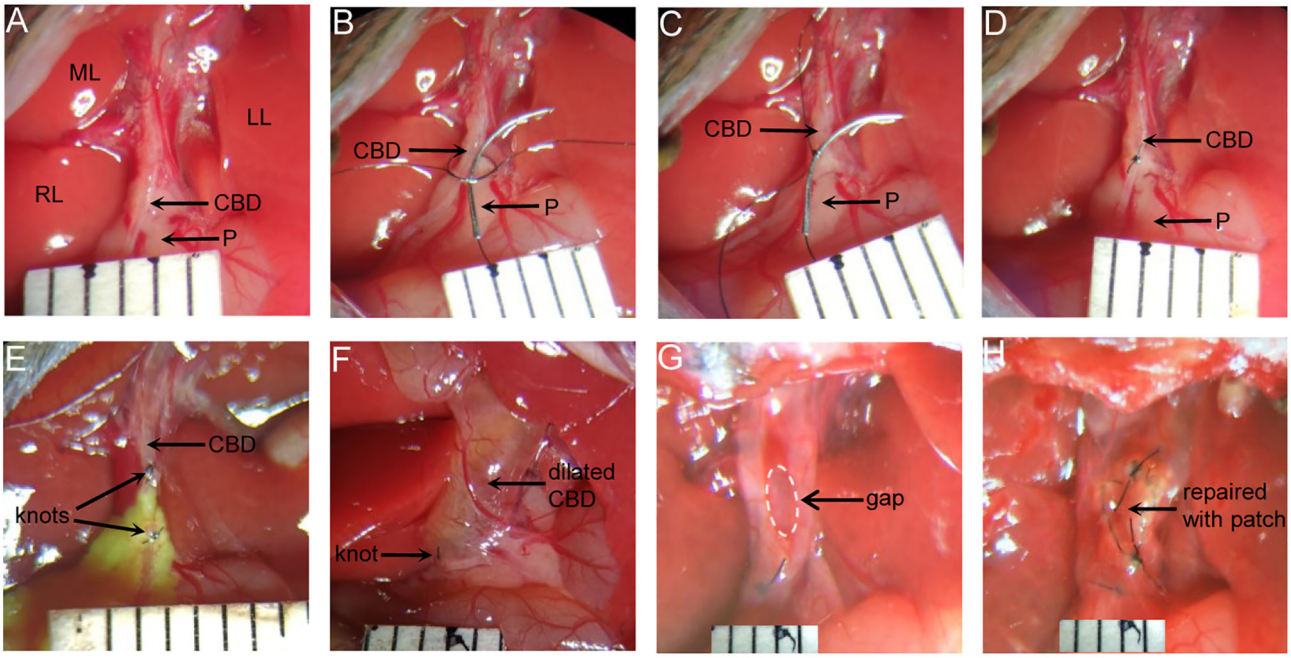

Figure 2. Intraoperative images of (A-D) BDD, (E) BDL and surgical repair of the injury at the dilated (F-H) CBD in mice. The scale of the white ruler is 1 mm. (A) The CBD of mice was exposed. (B) A loose knot was tied with an 8-0 nylon suture around the CBD and an 8-0 surgical needle was placed in the knot. (C) The surgical knot was tied tightly. (D) The needle was removed and partial ligation of the CBD was completed. (E) Double ligation of the CBD with 8-0 nylon suture and transection between the two knots. (F) The dilated CBD of BDD model mice was exposed and the knot for partial ligation was still visible. (G) One elliptical incision (shown with a white dotted line) was created on the ventral side. (H) The incision was repaired with a trimmed graft patch by continuous sutures. BDD, bile duct dilation; BDL, bile duct ligation; CBD, common bile duct; RL, right liver lobe; ML, middle liver lobe; LL, left liver lobe; P, pancreas.

Samples of liver tissue were fixed with 10% buffered formalin at 4˚C for 24 h. Finally, the mice were sacrificed by exsanguination. Prior to sample collection, a high-resolution small animal ultrasound system (Vevo 2100, VisualSonics) was also used for the noninvasive measurement of CBD diameter in the BDD group mice 21 days after the operation.

Blood biochemical analysis. Levels of serum alanine aminotransferase (ALT), aspartate aminotransferase (AST) and total bilirubin (TBil) were measured using the Cobas 8000 serum analyzer (Roche Diagnostics).

Histology and immunofluorescence detection. The fixed bile duct and liver tissue were embedded in paraffin after dehydration in an ascending ethanol series in turn (from 75 to 100% ethanol), cleared by dimethylbenzene and cut into 5-μm thick sections. For hematoxylin and eosin (HE) staining, sections were stained for 3 min with hematoxylin and 1 min with eosin at room temperature. For assessment of the presence of collagen, the sections were stained with Masson's Trichrome including staining in Weigert hematoxylin for 8 min, Ponceau for 10 min and aniline blue for 2 min at 25˚C. For immunofluorescence detection, the bile duct was further fixed with 4% paraformaldehyde for 4 h at 4˚C, dehydrated with 30% sucrose solution and then embedded with OCT for 8-μm thick frozen sections. Tissue sections were incubated at 4˚C overnight with primary antibodies against the myofibroblast (activated fibroblast) marker α smooth muscle actin (α-SMA; cat. no. D4K9N; 1:200; Cell Signaling Technology, Inc.), proliferative cell nuclear antigen (Ki67; cat. no. D3B5; 1:400; Cell Signaling Technology, Inc.) and cholangiocyte-specific marker cytokeratin 19 (CK19; cat. no. ab52625; 1:400; Abcam). Then, the sections were incubated with fluorescent secondary antibodies (1:400; Alexa 594; cat. no. 711-585-152; Jackson ImmunoResearch Laboratories, Inc.) at 25˚C for 2 h. Cell nuclei were stained with DAPI at 25˚C for 10 min (MilliporeSigma).

Indocyanine green (ICG) fluorescence imaging. Bile excretion of ICG can be used for real-time visualization of biliary tract structure. The mice were anaesthetized with isoflurane (3% isoflurane for induction, 1.5% for maintenance). Following a midline incision, 0.5 mg/kg ICG was injected into the inferior vena cava. Fluorescence imaging of the liver, biliary tract and duodenum was observed intermittently with an ICG imager (Beijing Digital Precision Medicine Technology Co. Ltd.).

Statistical analysis. All data are expressed as the mean ± standard deviation. Statistical analyses were performed by SPSS 17.0 (SPSS, Inc.). The values between the two groups were compared with unpaired Student's t test. Comparisons of multiple groups were performed with Student-Newman-Keuls test for three groups and Turkey test for more than three groups after analysis of variance (ANOVA). $P<0.05$ was considered to indicate a statistically significant difference.

Results

Changes in body weight and CBD diameter of the model mice. The body weight of both BDD mice (19.39±1.64 g) and

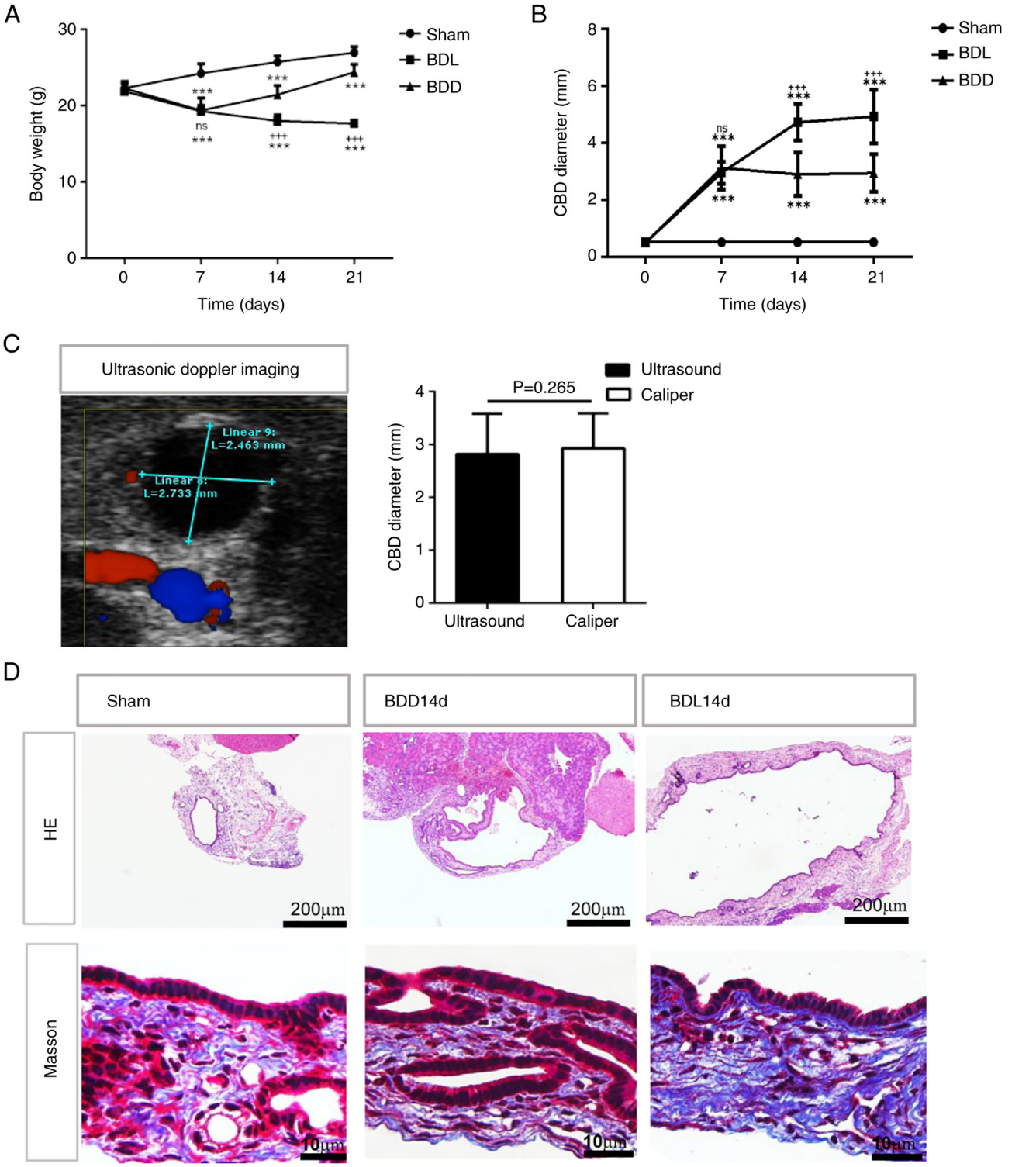

Figure 3. The changes in body weight and CBD of the mice that underwent different modelling operations. (A) The body weight of the Sham, BDL and BDD groups. (B) The CBD diameter of the Sham, BDL and BDD groups. (C) Representative ultrasonic Doppler imaging for the measurement of CBD diameter in the BDD mice on day 21 post operation compared with using the Vernier caliper method under laparotomy. (D) HE-stained CBD cross-sections and Masson staining for collagen in CBD cross-sections from sham, BDL and BDD mice on day 14 after the operation (magnification, x100). n=6 for the sham group; n=8 for the BDL and BDD groups. ***P<0.001 vs. Sham; $^{+++}$P<0.001 vs. BDD; ns, P>0.05 vs. BDD. CBD, common bile duct; BDL, bile duct ligation; BDD, bile duct dilation; HE, hematoxylin and eosin; ns, not significant.

BDL mice (19.30±0.79 g) decreased significantly during the first week postoperation compared with their baseline levels (BDD: 22.28±0.79 g; BDL: 21.89±1.08 g) or the Sham group (24.25±1.26 g; P<0.001). However, during the second and third weeks, the BDL mice continued to lose weight (day 14: 18.00±0.78 g; day 21: 17.40±0.53 g) and four mice had a body weight loss of >20% on day 21 and were sacrificed after sample collection. Meanwhile, the BDD mice began to gain weight (day 14: 21.46±1.18 g; day 21: 24.41±1.04 g) as did the Sham group mice (day 14: 25.75±0.82 g; day 21: 26.98±0.75 g;

Fig. 3A). The CBD diameter of sham mice was 0.51±0.08 mm. The CBD diameters of BDD mice were 3.11±0.76, 2.89±0.76 and 2.93±0.66 mm on days 7, 14 and 21 postoperation, respectively, while the CBD diameters of BDL mice were 2.95±0.39, 4.71±0.64 and 4.92±0.95 mm, respectively (Fig. 3B). The CBD remained slightly dilated in BDD mice but continued to expand in BDL mice from days 7 to 21 postoperation. These results indicated that the effect of partial CBD ligation on mouse body weight was transient and the degree of CBD dilation in BDD mice was mild and stable compared with that in BDL mice. To provide a noninvasive method to assess the degree of CBD dilation, the CBD diameter of BDD mice on day 21 was also measured with ultrasonic Doppler for small animals. As shown in Fig. 3C, the maximum bile duct diameter measured by ultrasonic Doppler was 2.82±0.77 mm, which was not significantly different from the diameter measured by Vernier calipers *in vivo* under laparotomy (2.93±0.66 mm, P=0.265). The bile duct diameters measured by the two methods were also comparable on days 7 and 14.

HE staining of the CBD cross sections also showed the mild expansion of CBD in the BDD group compared with the BDL group on day 14 (Fig. 3D). Masson staining showed a similar signal intensity for collagen in the Sham and BDD groups but much more compact collagen fiber deposition in the CBD wall of the BDL group. The thickness of the CBD wall was similar in the three groups and all had peribiliary glands within the CBD walls.

Liver function of the model mice. Complete CBD obstruction in BDL mice resulted in severe liver damage with markedly elevated ALT, AST and TBil serum levels and increased intrahepatic bile duct hyperplasia (as shown by HE staining and CK19 immunostaining) on days 7, 14 and 21 postoperation (Fig. 4). Nevertheless, the liver damage was very mild in BDD mice, with much lower ALT, AST and TBil serum levels and slight intrahepatic bile duct hyperplasia due to appropriate partial CBD ligation (Fig. 4). As the CBD diameter and liver damage of BDD mice became stable from day 14 after the operation, Day 14 was chosen as the time point to perform bile duct injury and repair in BDD mice in the following experiments.

Outcomes of the mice with bile duct transplantation. The size of the elliptical incision made on the dilated CBD was 2.53±0.48 mm in length and 1.7±0.41 mm in width (n=6). The trimmed patch was 3.53±0.48 mm in length and 2.73±0.46 mm in width (n=6). Altogether, 34 BDD mice underwent bile duct transplantation (referred to as Tp mice); of these, 30 Tp mice survived to the scheduled time points without obvious morbidity or body weight loss. Three mice died of abdominal bleeding on the second day and one mouse succumbed on the seventh day due to bile leakage. These mice were excluded from the study.

The present study first examined the mice that survived 12 weeks after CBD repair. Under a surgical microscope, the position of the grafted patch could be roughly identified by the surgical suture (Fig. 5A). The patch was covered with abundant blood vessels and fused with the native CBD. The border was indistinguishable except for the suture. The CBD retained the same degree of dilation as when being repaired. There were no signs of bile leakage or intraabdominal abscesses in the Tp mice. Fluorescence imaging showed that ICG could be excreted from the liver through the CBD into the duodenum, indicating that the CBD was unobstructed (Fig. 5B).

Liver injury in Tp mice was examined at 1, 2, 4 and 12 weeks after CBD repair. Although their ALT and AST serum levels were slightly higher than those of the Sham group, they were comparable to or slightly higher than those before CBD repair (BDD14d). The TBil levels of the Tp mice at 1, 2 and 4 weeks after CBD repair were not significantly different from those before CBD repair (BDD14d) (Fig. 5C). HE staining showed that the hepatic sinus structure remained intact and there was slight bile duct hyperplasia in Tp mice, as shown by CK19 immunostaining (Fig. 5D). However, mild liver injury did not affect the long-term survival of Tp mice.

Histologic examination of the transplanted patches. The long-term outcomes of repaired CBD were examined by cross transplantation of bile duct patches from EGFP mice to wild-type mice and vice versa at 12 weeks after transplantation. As shown in Fig. 6, HE staining showed that the CBD structure was intact and its lumen was free from sludge. Immunofluorescence detection of cholangiocyte marker CK19 showed that the $CK19^+$ biliary epithelium on the bile duct patch, which was identified by the surgical suture, was arranged in an orderly manner. There were peribiliary glands (PBGs) that were $CK19^+$ within the bile duct wall of the patch and the native bile duct (Fig. 6A and B). However, no $EGFP^+$ cells were preserved within the patch from EGFP BDD mice (Fig. 6B) and vice versa, the patches became EGFP positive when the patches from wild-type mice were transplanted into EGFP BDD mice at 12 weeks after transplantation (Fig. 6C and D). These results demonstrated that the transplanted bile duct patch, including biliary epithelial cells, was replaced by recipient-derived cells.

Regeneration process of the repaired CBD. The regeneration process of the repaired CBD with EGFP patches was observed at 1, 2 and 4 weeks after transplantation. As shown in Fig. 7, at 1 week, there were still numerous EGFP-positive cells within the patch and the wall structure of the patch seemed intact with $CK19^+$ and $EGFP^+$ epithelium (indicated with a white arrow) and PBGs (indicated with a yellow arrow). At 2 weeks, the patch lost its $CK19^+$ epithelium and connected with a mass of loosely released substance protruding into the lumen of the CBD. Meanwhile, the structure of the patch seemed disordered in HE staining. However, at 4 weeks, the patch was again covered with $CK19^+$ biliary epithelium and the wall structure of the patch became ordered again. Only a few $EGFP^+$ and $CK19^+$ PBGs were still present within the bile duct wall in some mice. The loose material released from the patch into the lumen was obviously reduced or missing. During this repair process, the native CBD did not seem to change much and was always covered with $CK19^+$ biliary epithelium. These results suggested that the bile duct patch went through a process from destruction to regeneration and its cells were replaced by recipient-derived cells, including biliary epithelial cells.

Regeneration mechanism of the transplanted CBD patch. Ki67 is a commonly used sensitive indicator of cell proliferation.

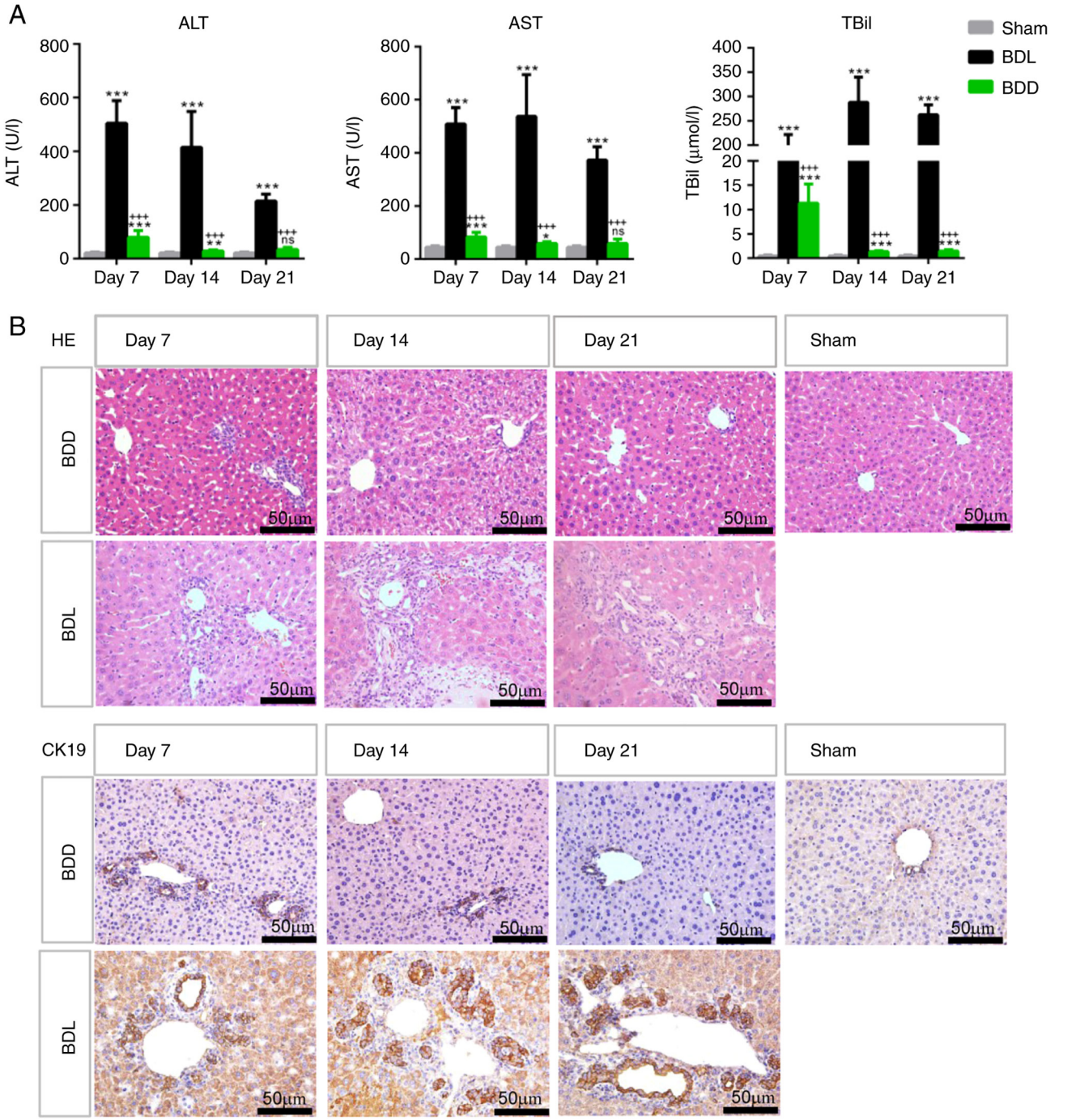

Figure 4. The liver function of the mice that underwent different modelling operations. (A) ALT, AST and TBil serum levels in the Sham, BDL and BDD groups on days 7, 14 and 21 after the operation. n=6 for the Sham group, n=8 for the BDL and BDD groups. *P<0.05 vs. sham; **P<0.01 vs. sham; ***P<0.001 vs. Sham; $^{+++}$P<0.001 vs. BDL; ns, P>0.05 vs. Sham. (B) HE staining and CK19 immunostaining of liver sections from Sham, BDL and BDD mice (magnification, x400). ALT, alanine aminotransferase; AST, aspartate aminotransferase; TBil, total bilirubin; BDD, bile duct dilation; BDL, bile duct ligation; HE, hematoxylin and eosin.

Immunofluorescence staining of the repaired CBD indicated that a significantly increased number of Ki67^{+} cells was observed within and adjacent to the patch compared with the native CBD at 1, 2 and 4 weeks following transplantation, demonstrating the activation of cell proliferation during the repair process (Fig. 8). In the patch, Ki67^{+} cuboidal columnar epithelial cells were found within the biliary epithelium and peribiliary glands identified by neatly arranged tall columnar nuclei (indicated with a white arrow). The cell proliferation of the biliary epithelium was most significant at 2 weeks after transplantation. There were almost no Ki67^{+} cells in the patch at 12 weeks after transplantation.

α-SMA is usually used as a marker of myofibroblasts or activated fibroblasts. An increase in α-SMA^{+} cells was also observed during the regeneration process of repaired CBD (Fig. 9). Immunofluorescence staining for α-SMA indicated significantly upregulated expression in the patch compared with the native CBD at 1, 2 and 4 weeks after transplantation.

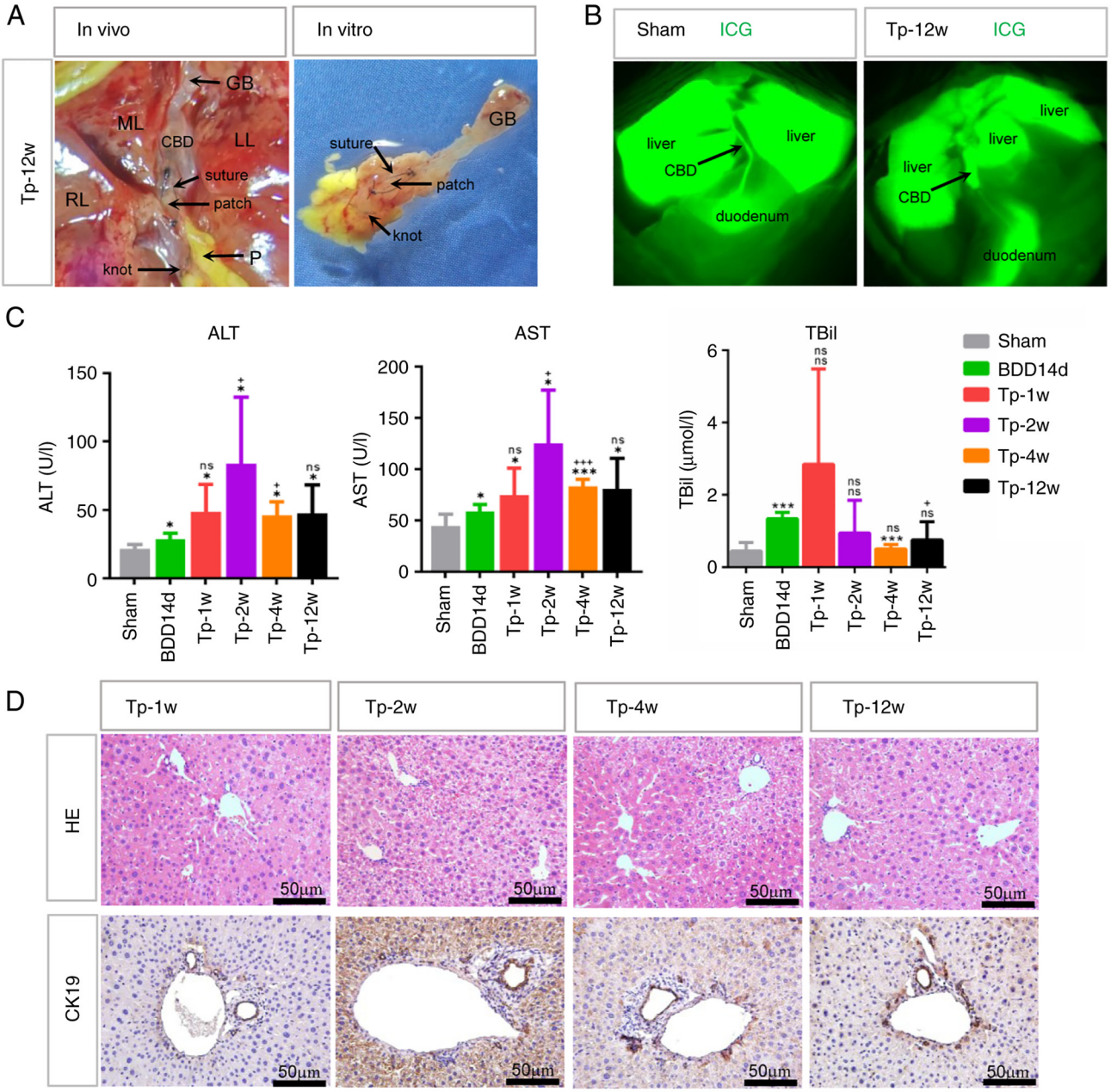

Figure 5. The macroscopic finding of repaired CBD and liver function of BDD mice following transplantation of bile duct patches (Tp mice). (A) Images of the repaired CBD *in situ* and *in vitro* from the Tp mice 12 weeks after transplantation under a surgical microscope (magnification, x10). (B) ICG fluorescence imaging of sham mice and Tp mice 12 weeks after transplantation showing that ICG was excreted from the liver through the CBD into the duodenum. (C) ALT, AST and TBil serum levels in BDD mice before (BDD14d) and 1, 2, 4 and 12 weeks after transplantation. n=6 for each time point of each group. *P<0.05 vs. sham; ***P<0.001 vs. Sham; $^{+}$P<0.05 vs. BDD14d; $^{+++}$P<0.001 vs. BDD14d; ns, P>0.05 vs. sham or BDD14d. (D) HE staining and CK19 immunostaining of representative liver sections showing mild bile duct hyperplasia in Tp mice (magnification, x400). CBD, common bile duct; BDD, bile duct dilation; ICG, indocyanine green; ALT, alanine aminotransferase; AST, aspartate aminotransferase; TBil, total bilirubin; HE, hematoxylin and eosin; ns, non significant.

The increase in α-SMA expression was highest at 2 weeks after transplantation. At 12 weeks, the α-SMA expression level in the patch was comparable to that in the native CBD. These results suggested that the regeneration of the muscular layer and epithelia occurred at the same rate to complete the CBD repair process.

Discussion

The outcomes of the current treatment strategies for bile duct injury are not always favorable (2,3). Much remains to be clarified with regard to the process of bile duct healing or regeneration following severe injury. The present study investigated whether a bile duct defect and repair model could be established in mice, which are the most commonly used animal models for studying mechanisms. The present study successfully established a novel mouse model for the study of bile duct injury and repair. To the best of the authors' knowledge, this is the first study to report the histological changes and healing process of repaired CBD.

For BDL model, it is important to ensure that the CBD is ligated by two surgical knots and then transected between

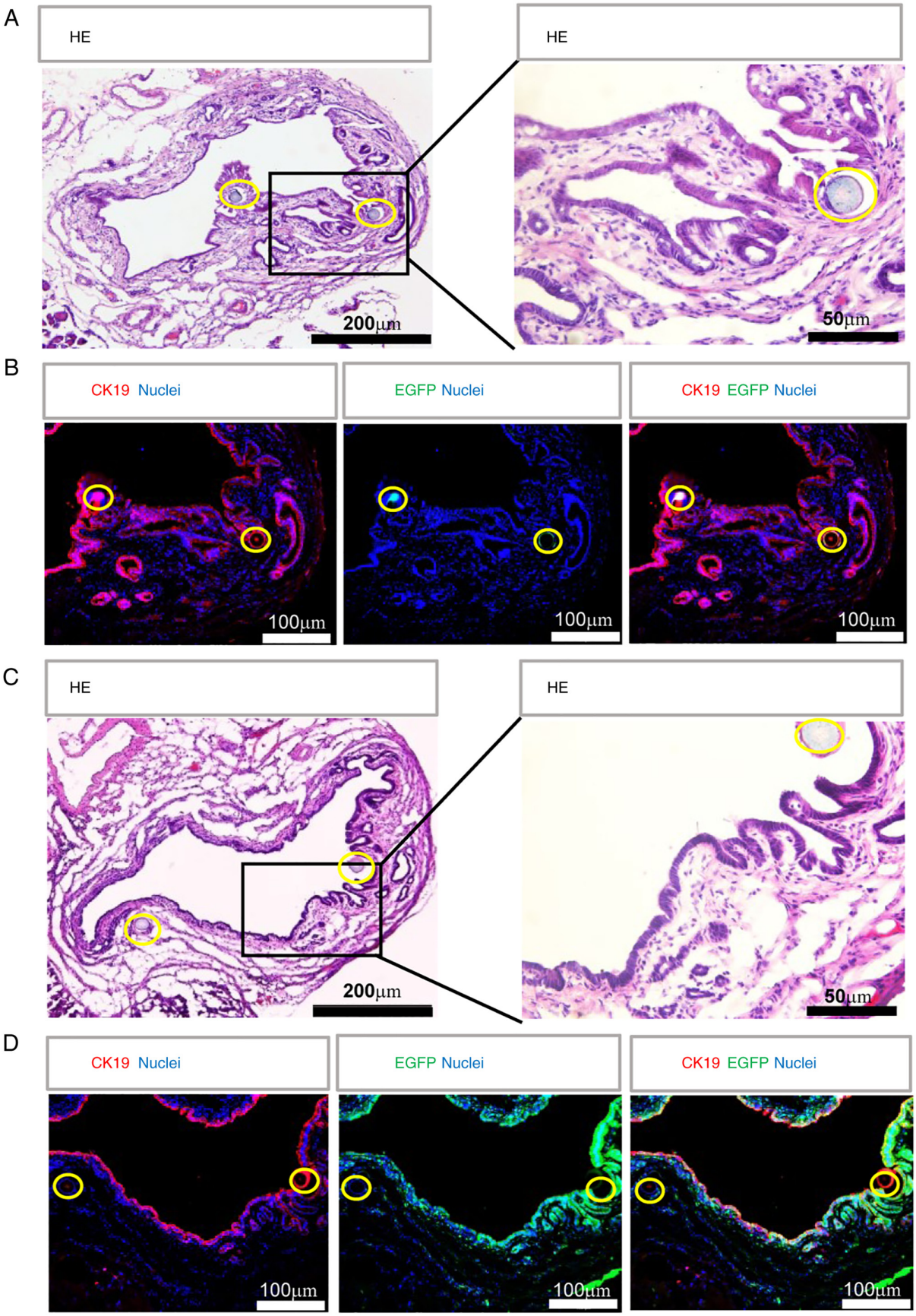

Figure 6. The bile duct patches were replaced by recipient-derived cells at 12 weeks after transplantation. The CBD of wild-type BDD mice repaired with bile duct patches from EGFP$^+$ mice. (A) HE staining showed the position of the patch and the repaired intact CBD. (B) Immunofluorescence staining of CK19 showed that the biliary epithelium and peribiliary glands were CK19+ and no EGFP+ cells were observed. (C) HE staining of the CBD of EGFP BDD mice repaired with bile duct patches from wild-type mice. (D) Immunofluorescence staining of CK19 showed that the biliary epithelium of the CBD was positive for both CK19 and EGFP. Yellow circles indicate the sutures and the patch was between the two sutures. CBD, common bile duct; BDD, bile duct dilation; HE, hematoxylin and eosin; EGFP, enhanced green fluorescence protein.

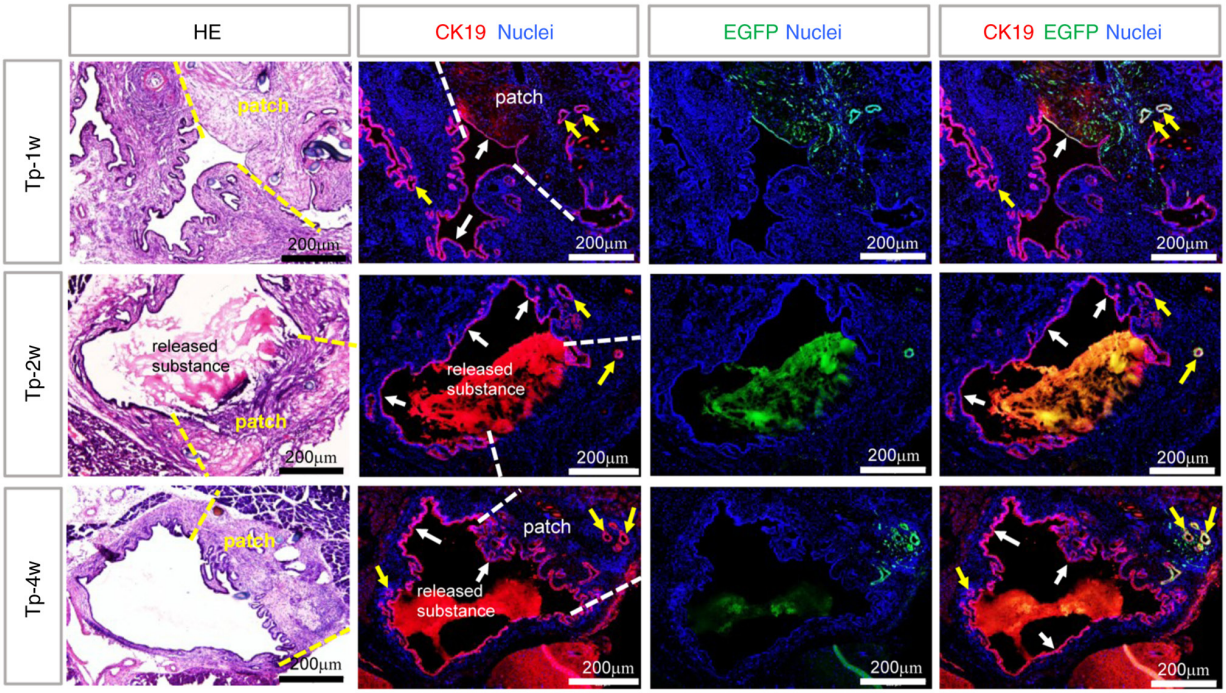

Figure 7. HE and immunofluorescence staining showing the regeneration process of the injured CBD of wild-type mice. Yellow- and white-dashed lines indicate the locations of the patches. CK19 immunofluorescence staining showing the biliary epithelium (white arrow) and PBGs (yellow arrow) of the patches and native CBDs. EGFP$^+$ donor cells of the patch were replaced by the recipient-derived EGFP$^-$ cells. HE, hematoxylin and eosin; CBD, common bile duct; PBG, peribiliary gland; EGFP, enhanced green fluorescence protein.

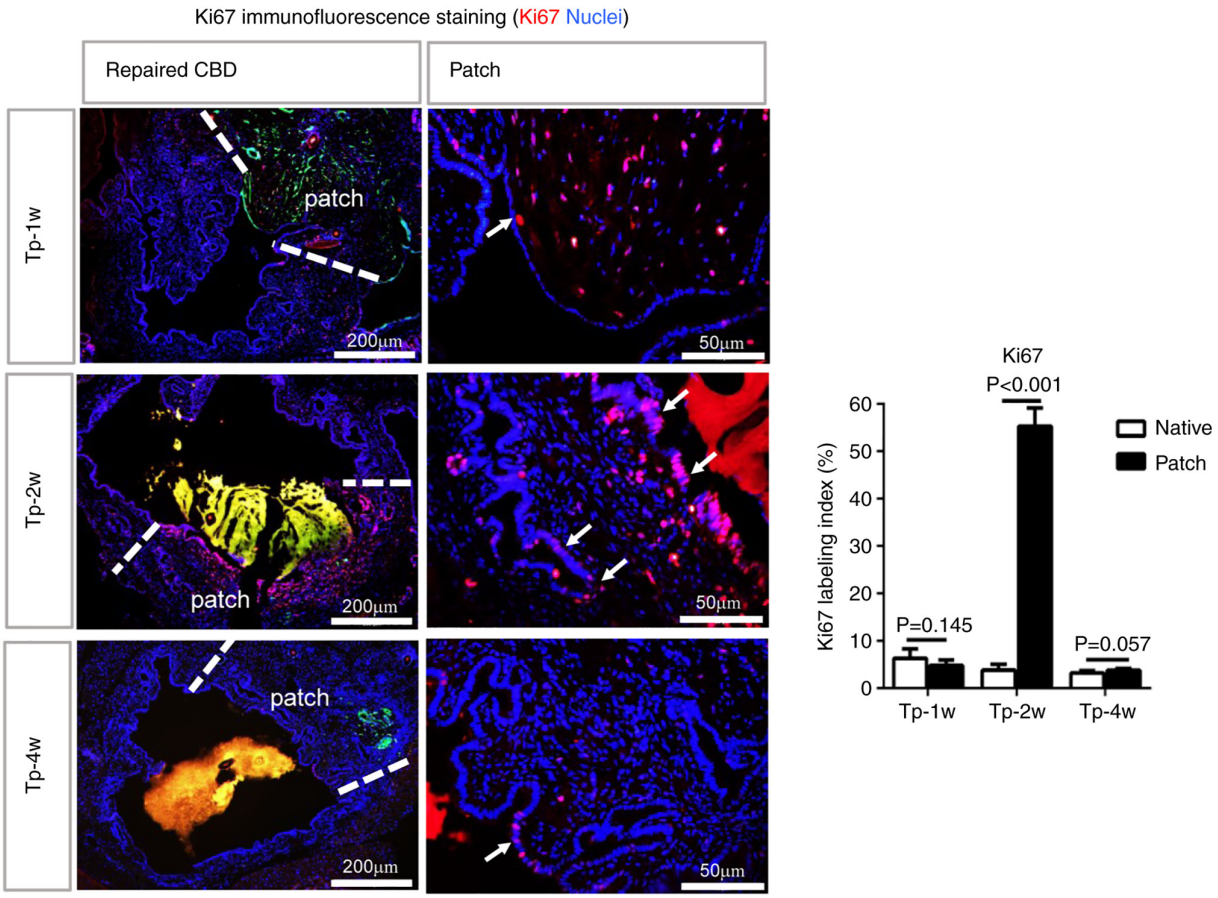

Figure 8. Immunofluorescence staining for the proliferative cell marker Ki67 in frozen sections of repaired CBD at 1, 2 and 4 weeks after transplantation. More Ki67$^+$ cells were present in the patch than in the native CBD (white dashed lines indicate the margin of the patches). In the patch, Ki67$^+$ cuboidal columnar epithelial cells were observed within the epithelium and peribiliary glands were identified by neatly arranged tall columnar nuclei (white arrow). Semiquantitative evaluation of the Ki67 labelling index of the epithelium. CBD, common bile duct.

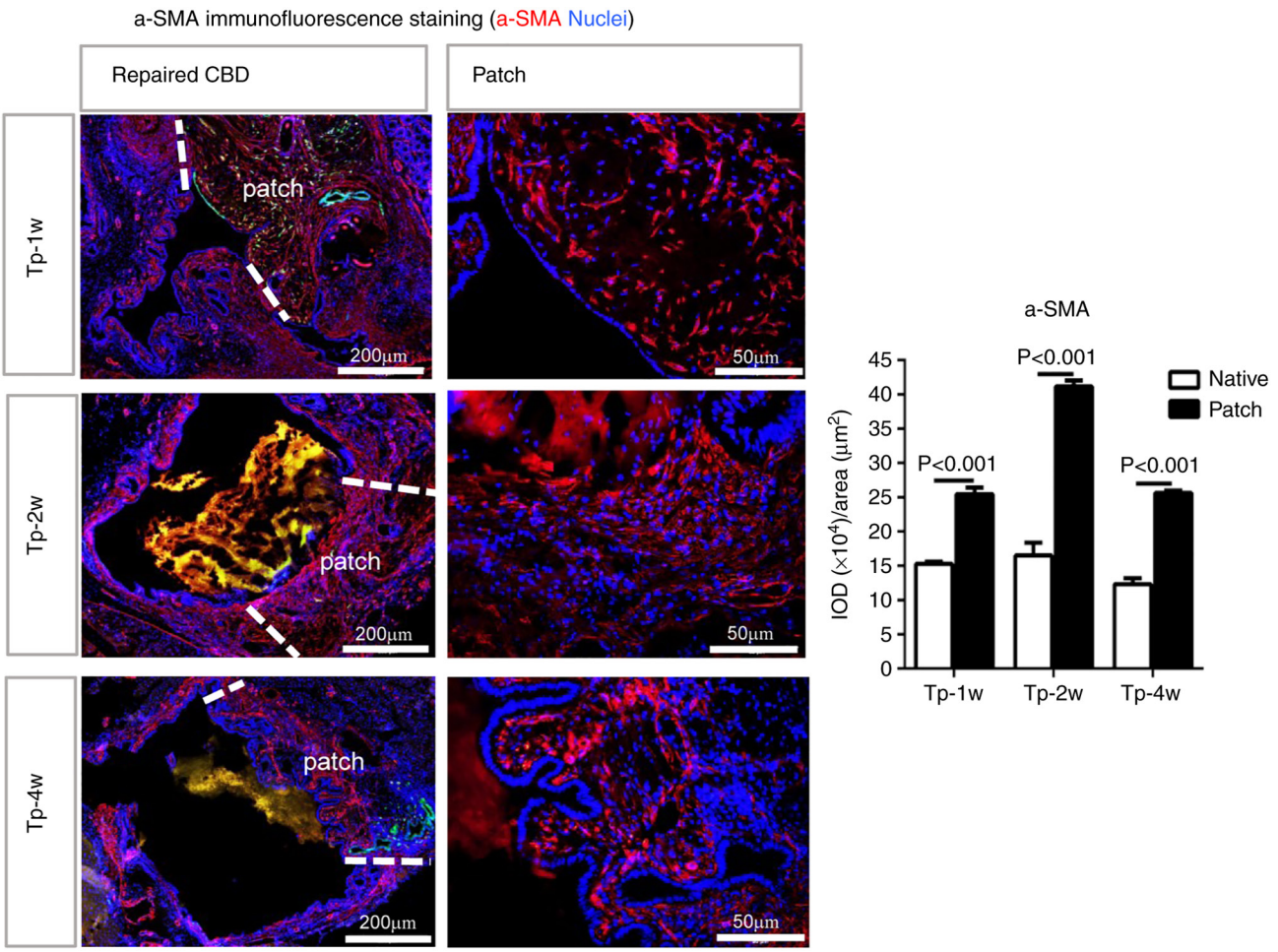

Figure 9. Immunofluorescence staining for α-SMA in frozen sections of the repaired CBD at 1, 2 and 4 weeks after transplantation. α-SMA expression was significantly higher in the patch than in the native CBD and was most obvious at 2 weeks after transplantation (white dashed lines indicate the margin of the patches). Semiquantitative evaluation of α-SMA expression. α-SMA, α smooth muscle actin; CBD, common bile duct.

the two ligations (17,18). One of the key points of BDD mouse model is the proper induction of CBD dilation by partial ligation of the CBD, which makes the slender bile duct of the mouse moderately dilated for easier surgical repair. Although the BDD mice experienced obvious but mild liver injury because of biliary stenosis compared with the Sham group, its effect on body weight was transient and the BDD mice did not show obvious morbidity. In BDL mice where the CBD was completely obstructed, their body weight decreased dramatically, their liver damage was very serious and their ALT, AST and TBil levels were 10 times higher than those of BDD mice. BDL caused a decrease in body weight by ~20% and obvious liver injury which were also observed in previous studies (19,20). In the study by Heinrich *et al* (14), a similar method was used to establish a model of acute cholestasis in mice; however, the gallbladder was removed and the mice were observed for only 2 weeks in their study. In the present BDD model, the gallbladder was preserved to maintain the physiological state as much as possible and the gallbladders of BDD mice did not show obvious expansion, in contrast to the extensively expanded gallbladder in BDL mice. These BDD mice survived at least 6 months without significant symptoms of morbidity.

The CBD diameter of normal mice was ~0.5 mm. After BDD, the CBD became 4-7-fold of its normal size and reached a steady state from day 14 after surgery. HE and Masson staining showed that the CBD wall of BDD mice was similar to that of normal mice, but there was more collagen fiber in the CBD wall of BDL mice. This might be due to the high biliary pressure because of complete obstruction in the BDL mice. These results suggested that the degree of bile duct dilation in the BDD model was very mild and had little effect on its survival.

The present study then demonstrated that the dilated CBD could be injured and repaired easily by suturing a bile duct patch onto the damaged region under surgical microscopy. It is almost impossible to perform these procedures on normal mice. Biliary fistula was the main reason for early mortality and usually occurred during the learning period for the micro-surgical performer. After a short time of training, >90% of the mice were able to survive to the predetermined time points.

In addition, the CBD diameter remained almost the same as before repair during the observation period of 12 weeks, although it was not accurately measured because of tissue adhesion. There were no signs of bile leakage or intraabdominal abscesses. At 12 weeks, the site of the patch was covered with abundant blood vessels and was indistinguishable from the native duct. Its lumen was free from sludge. Histological examination also demonstrated that the bile duct injury was completely repaired

and could not be distinguished from the surrounding CBD wall. Only the suture silk could show the approximate position of the patch. The suture silk was even extruded into the lumen from the bile duct wall after 6 months (data not shown).

By cross transplantation of the bile duct patch between wild-type mice and EGFP mice, it was found that no $EGFP^+$ cells were observed within the patch at 12 weeks after transplantation when the EGFP patch was transplanted into wild-type mice and vice versa, the site of the patch became $EGFP^+$ when the wild-type mouse patch was transplanted into EGFP mice. At 1 week after transplantation, the biliary epithelium of the patch seemed intact and there were still numerous $EGFP^+$ cells in the patch. However, at 2 weeks after transplantation, $EGFP^+$ cells were destroyed and reduced and the biliary epithelium became imperfect. At 4 weeks, the biliary epithelium regenerated and became intact. $CK19^+$ $EGFP^-$ cholangiocytes with tall columnar nuclei were neatly arranged on the inner side of the CBD, although a few $EGFP^+$ peribiliary glands were still present within the CBD wall in some mice. These results demonstrated that the transplanted bile duct patch, including the biliary epithelium, was replaced by recipient-derived cells. The injured CBD was regenerated and repaired. Recently, de Jong *et al* (11) also demonstrated that recipient-derived cholangiocytes were present in the large bile ducts of the donor liver after liver transplantation. The presence of chimaerism in the large bile ducts suggested that recipient-derived cells may play a role in biliary regeneration following ischemia-induced injury.

The regeneration of transplanted artificial bile ducts at the graft site after the tube had been degraded has been reported in several experimental studies in pigs (21,22), but the detailed process was not disclosed. The present study demonstrated that the transplanted bile duct patch did not survive but went through a process of destruction and regeneration. It is known that epithelial cells and periductal myofibroblasts are closely linked because damage to the former leads to activation and proliferation of the latter (23,24). $Ki67^+$ cuboidal columnar epithelial cells were found within the columnar biliary epithelial and peribiliary glands. An increase in α-SMA^+ myofibroblasts was also observed in the bile duct wall of the patch and the surrounding area. The proliferation was most significant at 1-4 weeks after the repair operation. At 12 weeks, the number of Ki67-positive cells was minimal and the number of α-SMA^+ cells was reduced to the level observed in the surrounding bile duct wall. These results were consistent with the process of graft re-epithelialization observed by HE and CK19 staining. Although it was not clear whether the extracellular matrix was also completely replaced by new extracellular matrix, synthesis of extracellular matrix by α-SMA^+ cells was suggested.

Long-term outcomes are key clinical settings for the surgical treatment of bile duct injury. A satisfactory follow-up period of 2-5 years is necessary to assess the long-term outcome of repair surgery (2,3). In the present study, 12 weeks is a relatively long time considering the lifespan of mice. Creation of artificial bile ducts functionally identical to natural organs is a final goal in the research area of artificial bile ducts. In the study of Sampaziotis *et al* (7), the bile ducts were repaired using specially made very fine artificial tissue-engineered bile ducts and the microsurgical procedure was extremely difficult and lacked universality. In the present study, a BDD model was used to achieve bile duct injury and repair in mice, which significantly reduced the difficulty of microsurgery. It was hypothesized that the mouse model established in the present study can be used to evaluate the biocompatibility, repairing effect and mechanism of tissue-engineered bile ducts (8-10). Notably, if the survival of the grafted bile duct patch is not as important as proven in the present study, cryopreserved bile duct, allogeneic or even heterogenic decellular bile duct might be superior to synthetic materials for the recipient-derived cells to engraft after transplanting (25,26).

The limitation of the present study was that bile duct injury and repair were not performed in healthy mice but in an experimental model of partial bile duct ligation. However, when the bile duct needs to be repaired due to injury or stricture, it would also be carried out in a pathologic environment. Therefore, the BDD model has clinical significance. As the dilated CBD was short and stuck tightly together to the portal vein below, it was very easy to injure the portal vein when attempting to resect the stenosis at the beginning to establish this model. Therefore, due to technical reasons, the stenosis was not removed when the CBD was repaired in the present study. It is hoped to perform this with more elaborate microsurgical procedures or in other experimental animals, such as rats, in future studies. In addition, due to the small size of the bile duct patch, a limited number of tissue sections were available for immunofluorescence and IHC staining and the presence of EGFP fluorescence limited the double staining capabilities. Therefore, more detailed cellular and molecular analyses were not performed in this study.

To the best of the authors' knowledge, this is the first study to show a replicable and successful model for the study of bile duct injury and repair in mice. With the help of surgical microscopy, a good postoperative survival rate (>90%) was obtained in the present study without serious complications. Preliminary results suggested that the recipient-derived cells were responsible for bile duct repair through epithelial cell proliferation and extracellular matrix synthesis. More elaborate molecular mechanisms of bile duct injury and repair will be explored using genetically engineered mice or cell tracer techniques in the future.

Acknowledgements

Not applicable.

Funding

This research was funded by the Nonprofit Industry Research Project of National Health Commission (grant no. 201502014); National Natural Science Foundation of China (81670590); National Key R&D Program of China (grant nos. 2017YFA0103003 and 2017YFA0103002).

Availability of data and materials

The datasets used and/or analyzed during the current study are available from the corresponding author on reasonable request.

Authors' contributions

XG and DX participated in the experiments and were responsible for the data acquisition and analysis. KP and GM were responsible for literature searches and statistical analysis. XG and CL drafted the manuscript. CL and SL designed the study. XG and CL confirm the authenticity of all the raw data. All authors read and approved the final manuscript.

Ethics approval and consent to participate

Experiments were approved by the Committee on Ethics of Animal Experiments of the Chinese PLA General Hospital (approval no. 2017-X13-65) and in compliance with the recommendations of the Guide for the Care and Use of Laboratory Animals of the National Research Council (US) Committee, 8th edition, 2011 (https://nap.nationalacademies.org/read/12910).

Patient consent for publication

Not applicable.

Competing interests

The authors declare that they have no competing interests.

References

1. Pesce A, Palmucci S, La Greca G and Puleo S: Iatrogenic bile duct injury: Impact and management challenges. Clin Exp Gastroenterol 12: 121-128, 2019.
2. Booij KAC, Coelen RJ, de Reuver PR, Besselink MG, van Delden OM, Rauws EA, Busch OR, van Gulik TM and Gouma DJ: Long-term follow-up and risk factors for strictures after hepaticojejunostomy for bile duct injury: An analysis of surgical and percutaneous treatment in a tertiary center. Surgery 163: 1121-1127, 2018.
3. Booij KAC, de Reuver PR, van Dieren S, van Delden OM, Rauws EA, Busch OR, van Gulik TM and Gouma DJ: Long-term impact of bile duct injury on morbidity, mortality, quality of life, and work related limitations. Ann Surg 268: 143-150, 2018.
4. Stilling NM, Fristrup C, Wettergren A, Ugianskis A, Nygaard J, Holte K, Bardram L, Sall M and Mortensen MB: Long-term outcome after early repair of iatrogenic bile duct injury. A national Danish multicentre study. HPB (Oxford) 17: 394-400, 2015.
5. Tocchi A, Mazzoni G, Liotta G, Lepre L, Cassini D and Miccini M: Late development of bile duct cancer in patients who had biliary-enteric drainage for benign disease: A follow-up study of more than 1,000 patients. Ann Surg 234: 210-214, 2001.
6. Buisson EM, Jeong J, Kim HJ and Choi D: Regenerative medicine of the bile duct: Beyond the myth. Int J Stem Cells 12: 183-194, 2019.
7. Sampaziotis F, Justin AW, Tysoe OC, Sawiak S, Godfrey EM, Upponi SS, Gieseck RL III, de Brito MC, Berntsen NL, Gómez-Vázquez MJ, *et al*: Reconstruction of the mouse extrahepatic biliary tree using primary human extrahepatic cholangiocyte organoids. Nat Med 23: 954-963, 2017.
8. Justin AW, Saeb-Parsy K, Markaki AE, Vallier L and Sampaziotis F: Advances in the generation of bioengineered bile ducts. Biochim Biophys Acta Mol Basis Dis 1864: 1532-1538, 2018.
9. Miyazawa M, Aikawa M, Okada K, Toshimitsu Y, Okamoto K, Koyama I and Ikada Y: Regeneration of extrahepatic bile ducts by tissue engineering with a bioabsorbable polymer. J Artif Organs 15: 26-31, 2012.
10. Zeng J, Wang J, Dong J, Huang X, Xia H and Xiang X: The application of vascularized stomach flap to repair postoperative biliary stricture. Medicine (Baltimore) 97: e11344, 2018.
11. de Jong IEM, Sutton ME, van den Heuvel MC, Gouw ASH and Porte RJ: Evidence for recipient-derived cells in peribiliary glands and biliary epithelium of the large donor bile ducts after liver transplantation. Front Cell Dev Biol 8: 693, 2020.
12. Lee J, Chan MC, James C and Lantis JC II: Cryopreserved allograft use in vascular surgery. Surg Technol Int 37: 237-243, 2020.
13. Furlough CL, Jain AK, Ho KJ, Rodriguez HE, Tomita TM and Eskandari MK: Peripheral artery reconstructions using cryopreserved arterial allografts in infected fields. J Vasc Surg 70: 562-568, 2019.
14. Heinrich S, Georgiev P, Weber A, Vergopoulos A, Graf R and Clavien PA: Partial bile duct ligation in mice: A novel model of acute cholestasis. Surgery 149: 445-451, 2011.
15. Talbot SR, Biernot S, Bleich A, van Dijk RM, Ernst L, Häger C, Helgers SOA, Koegel B, Koska I, Kuhla A, *et al*: Defining body-weight reduction as a humane endpoint: A critical appraisal. Lab Anim 54: 99-110, 2020.
16. Emond J, Capron-Laudereau M, Meriggi F, Bernuau J, Reynes M and Houssin D: Extent of hepatectomy in the rat. Evaluation of basal conditions and effect of therapy. Eur Surg Res 21: 251-259, 1989.
17. Chilvery S, Bansod S, Saifi MA and Godugu C: Piperlongumine attenuates bile duct ligation-induced liver fibrosis in mice via inhibition of TGF-β1/Smad and EMT pathways. Int Immunopharmacol 88: 106909, 2020.
18. Tang G, Seume N, Häger C, Kumstel S, Abshagen K, Bleich A, Vollmar B, Talbot SR, Zhang X and Zechner D: Comparing distress of mouse models for liver damage. Sci Rep 10: 19814, 2020.
19. Gäbele E, Froh M, Arteel GE, Uesugi T, Hellerbrand C, Schölmerich J, Brenner DA, Thurman RG and Rippe RA: TNFalpha is required for cholestasis-induced liver fibrosis in the mouse. Biochem Biophys Res Commun 378: 348-353, 2009.
20. Ezure T, Sakamoto T, Tsuji H, Lunz JG III, Murase N, Fung JJ and Demetris AJ: The development and compensation of biliary cirrhosis in interleukin-6-deficient mice. Am J Pathol 156: 1627-1639, 2000.
21. Aikawa M, Miyazawa M, Okamoto K, Toshimitsu Y, Torii T, Okada K, Akimoto N, Ohtani Y, Koyama I and Yoshito I: A novel treatment for bile duct injury with a tissue-engineered bioabsorbable polymer patch. Surgery 147: 575-580, 2010.
22. Zong C, Wang M, Yang F, Chen G, Chen J, Tang Z, Liu Q, Gao C, Ma L and Wang J: A novel therapy strategy for bile duct repair using tissue engineering technique: PCL/PLGA bilayered scaffold with hMSCs. J Tissue Eng Regen Med 11: 966-976, 2017.
23. Siqueira OH, Herani Filho B, Paula RE, Ascoli FO, Nóbrega AC, Carvalho AC, Pires AR, Gaglionone NC, Cunha KS and Granjeiro JM: Tamoxifen decreases the myofibroblast count in the healing bile duct tissue of pigs. Clinics (Sao Paulo) 68: 101-106, 2013.
24. Kosmidis C, Efthimiadis C, Anthimidis G, Basdanis G, Apostolidis S, Hytiroglou P, Vasiliadou K, Prousalidis J and Fahantidis E: Myofibroblasts and colonic anastomosis healing in Wistar rats. BMC Surg 11: 6, 2011.
25. Guruswamy Damodaran R and Vermette P: Tissue and organ decellularization in regenerative medicine. Biotechnol Prog 34: 1494-1505, 2018.
26. Roelofs LA, Oosterwijk E, Kortmann BB, Daamen WF, Tiemessen DM, Brouwer KM, Eggink AJ, Crevels AJ, Wijnen RM, van Kuppevelt TH, *et al*: Bladder regeneration using a smart acellular collagen scaffold with growth factors VEGF, FGF2 and HB-EGF. Tissue Eng Part A 22: 83-92, 2016.